MATHEMATICAL BIOSCIENCES
AND ENGINEERING
Volume **6**, Number **3**, July **2009**

doi:10.3934/mbe.2009.6.493

pp. **493–508**

NOVEL DESIGN OF DRUG DELIVERY IN STENTED ARTERIES: A NUMERICAL COMPARATIVE STUDY

Mario Grassi

Dept. of Chemical Engineering
University of Trieste, Italy

Giuseppe Pontrelli

Istituto per le Applicazioni del Calcolo
CNR, Roma, Italy

Luciano Teresi

Dept. of Structures
University of Roma Tre, Roma, Italy

Gabriele Grassi

Dept. of Life Science
University of Trieste, Italy

Lorenzo Comel, Alessio Ferluga and Luigi Galasso

Dept. of Material Engineering
University of Trieste, Italy

(Communicated by Mette S. Olufsen)

Abstract. Implantation of drug eluting stents following percutaneous transluminal angioplasty has revealed a well established technique for treating occlusions caused by the atherosclerotic plaque. However, due to the risk of vascular re-occlusion, other alternative therapeutic strategies of drug delivery are currently being investigated. Polymeric endoluminal pave stenting is an emerging technology for preventing blood erosion and for optimizing drug release. The classical and novel methodologies are compared through a mathematical model able to predict the evolution of the drug concentration in a cross-section of the wall. Though limited to an idealized configuration, the present model is shown to catch most of the relevant aspects of the drug dynamics in a delivery system. Results of numerical simulations shows that a bi-layer gel paved stenting guarantees a uniform drug elution and a prolonged perfusion of the tissues, and remains a promising and effective technique in drug delivery.

1. **Introduction.** Percutaneous transluminal angioplasty has been used in the past to treat coronary occlusion (stenosis) due to atherosclerotic plaques. However, the frequent occurrence of re-occlusion (restenosis) of the treated vessel observed after intervention [2] indicated the requirement of alternative approaches. The use of bare-metal stents (Fig. 1), rigid scaffolds placed in the artery lumen at the site of stenosis, has significantly improved the clinical outcome of treated patients without,

2000 *Mathematics Subject Classification.* Primary: 92B05, 62P10; Secondary: 74S05.

Key words and phrases. arterial stenting, drug delivery, mathematical modelling, numerical methods, finite elements.

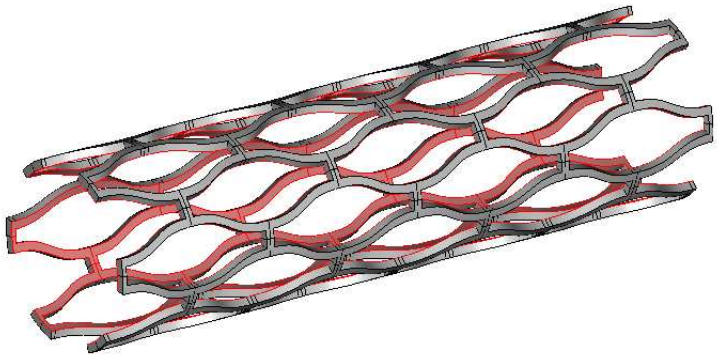

FIGURE 1. Typical stent structure (courtesy of Comsol).

however, solving the problem. Indeed, an inconvenience of these devices consists of the frequent induction of the exuberant proliferation of coronary smooth muscle cells (CSMCs), a phenomenon which ultimately determines the re-occlusion of the treated vessel (in-stent restenosis) [7, 22]. This problem has been substantially attenuated by the use of drug eluting stents (DES), which are able to deliver in situ antiproliferative drugs [1]. Although different configurations can exist, typically DES consists of one or more biocompatible polymeric coatings surrounding stent strut and containing the therapeutic agent to be delivered (Figs. 2 and 3a). Release rate basically depends on the complex combination of effects such as coating geometrical (thickness, for example) and physico-chemical properties and on drug characteristics such as diffusivity and coating-wall interaction. Accordingly, drug delivery can be controlled either by diffusion through the coating or by coating dissolution/degradation. In addition, while the drug can be dispersed in the coating (matrix configuration), it can be contained in proper depots (reservoir configuration) realized in the stent strut and separated from the release environment by the coating. Obviously, in order to finely tune drug delivery, coating can be composed by two or more layers showing different characteristics and/or drug loading [1]. Notably, for practical reasons, almost the totality of DES has stent strut coated before use. Although the use of DES has greatly contributed to reduce restenosis, very recently some researchers evidenced possible problems connected to the use of traditional DES [17, 24, 25, 27]. These studies seem to suggest that different drugs/approaches should be considered as CSMCs proliferation inhibitors. For example, nucleic acid based drug (NABD) showed to be very promising at this purpose as they can down regulate CSMC proliferation by suppressing the expression of relevant cell cycle promoting genes [8, 12, 14, 16, 21]. Unfortunately, for their fragile nature and for the fact that cellular internalization requires their complexation with transfection agents such as liposomes [9], NABD cannot be released by traditional DES and alternative delivery systems are considered.

The endoluminal gel paving technique (EGP) [23] in conjunction with implantation of an uncoated stent (devoted to hinder artery stenosis due to elastic recoil) is deemed an effective promising approach. The advantages of gel paving technique consist in i) an easy and safe complex (transfection agent-NABD) loading within the gel matrix and ii) in the possibility of creating a physical barrier between the

damaged artery wall and the overflowing thrombogenic and inflammatory elements present in the blood stream [23, 26]. Fundamental prerequisites for the success of this procedure are the gel resistance to blood erosion and the realization of proper drug release kinetics toward artery wall. While the first issue requires the theoretical estimation of the wall shear stress exerted by the blood stream, the second one implies a theoretical study on drug release kinetics from our in situ delivery system composed by a bi-layer gel. This consists of a hard inner side directed towards blood flow, and of a soft outer side in contact with the arterial wall. The former layer is thought to resist blood flow erosion, protecting the soft gel, which releases the complexes (transfection agent-NABD) to the arterial wall where CSMCs, the target cells, reside. Additionally, the hard gel, characterized by a low permeability, prevents from a significant systemic release. Thus, the novel character of our approach consists in combining two traditional methodologies such as bare stenting and EGP for the controlled delivery of NABD. The proposed technology, named *endoluminal gel paved stenting* (EGPS), offers a viable alternative to DES and suggests a possible solution to restenosis.

The aim of this study is to develop a mathematical model able to compare the performances of traditional coated stents (Sect. 2) and of the proposed EGPS methodology (Sect. 3) with respect of drug release and residence times. Because of the several variables and parameters involved, an appropriate degree of simplification is necessary to discern the relevant features of the phenomena. Although the complexity of stent geometry would require the use of 3D models [18], nevertheless for comparative purposes simpler two-dimensional models give some useful hints on the basic physics and allow a systematic analysis on a wide range of parameters, provided the essential ingredients are retained. Moreover the simpler form of the governing equations clearly shows correlations among the several variables and material parameters, and gives a deeper insight on the transport process.

Results from numerical simulations (Sect. 4) show drug diffusion patterns over a cross-section of the arterial wall in both cases. They can be used to identify simple indexes or clinical indicators useful in drug delivery design and to optimize drug elution for a desired tissue concentration.

2. **The conventional drug-eluting stent.**

A drug-eluting stent (DES) is a metallic prosthesis (*strut*) implanted into the arterial wall and coated with a thin layer of biocompatible polymeric gel that encapsulates a therapeutic drug (*coating*). Such a drug, released in a controlled manner through a permeable membrane, is aimed at preventing a possible restenosis by virtue of its anti-proliferative action against smooth muscle cells. In the present work we are interested in the mechanism of drug elution into the arterial tissue due to diffusion. As a matter of fact any other effects, such as a possible decomposition of the polymeric matrix or mechanical effects, are neglected.

The degree of embedding of the stent strictly depends on the nature of the atherosclerotic plaque coating the arterial wall. In principle, two limit cases can occur: a) the plaque is composed by soft material where the stent is easily and completely inserted, b) the plaque is calcified and stent insertion is completely hindered. In the first case embedding is total and instantaneous while, in the second one, embedding never occurs. Actual positioning are in between these two limiting cases and individual, or pathological conditions can make the picture more complicate as the arterial wall is a dynamic structure that can alter its morphology

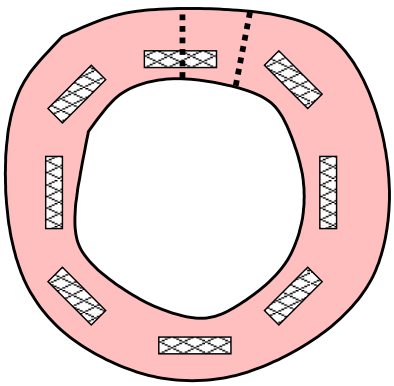

FIGURE 2. Schematic cross-section representation of a stented artery. The area between dashed lines constitutes the 2D computational domain, see Figure 3 (figure is not to scale).

in response to many external stimuli. Due to the complexity and uncertainty of this frame, the concept of *penetration depth* (named s) is used to explore possible scenarios occurring in relation with different insertion configurations. However s, though a model parameter, cannot be considered for design because it can not be controlled during stent implantation.

2.1. **Geometry.** Let us consider a stent coated by a thin layer of gel containing a drug and embedded into the arterial wall, as illustrated in Fig. 2. The complex multi-layered structure of the arterial wall has been disregarded and a homogeneous material with averaged properties has been considered for simplicity (*fluid-wall* model) as in [20]. Both the coating and the arterial wall are treated as porous media.

For the sake of simplicity, we restrict our study to a simplified 2D model and we assume the stent structure to be regular, having the width and the spacing of the meshes constant. As consequence, it is sufficient to consider a cross section of the wall and a slice of it containing a single strut Σ embedded into the wall at distance s from the endothelium (Fig 3a). In this idealized case, the full section of the stented artery is obtained from such a portion by circular symmetry and periodicity. Moreover, being the wall thickness very small with respect to the arterial radius, a cartesian coordinate system (x, y) is used on the tangential plane (Figs. 3).

We denote by l (resp. d) the width (resp. the thickness) of this rectangular portion of the wall, by L_x (resp. L_y) the half-length (resp. the thickness) of the strut embedded in it (the coating is supposed to be a thin layer around the strut of uniform thickness h_c). The strut represents a mechanical obstacle to the drug dynamics, while the wall and the coating constitute a coupled two-layered system where drug dynamics takes place. Such interfaced domains are denoted respectively by $\Sigma = [0, L_x] \times [s, s + L_y]$ (strut), Ω_c (coating) and $\Omega_w = [0, l] \times [0, d] \setminus (\Omega_c \cup \Sigma)$ (wall)[1] (Fig. 3a). Here, and throughout this paper, a concentration $c(x, t)$ $(\mu g/cm^2)$ is considered and a subindex is used for denoting the correspondent medium.

[1]In all the paper, subscript c (resp. w) refers to the coating (resp. to the wall).

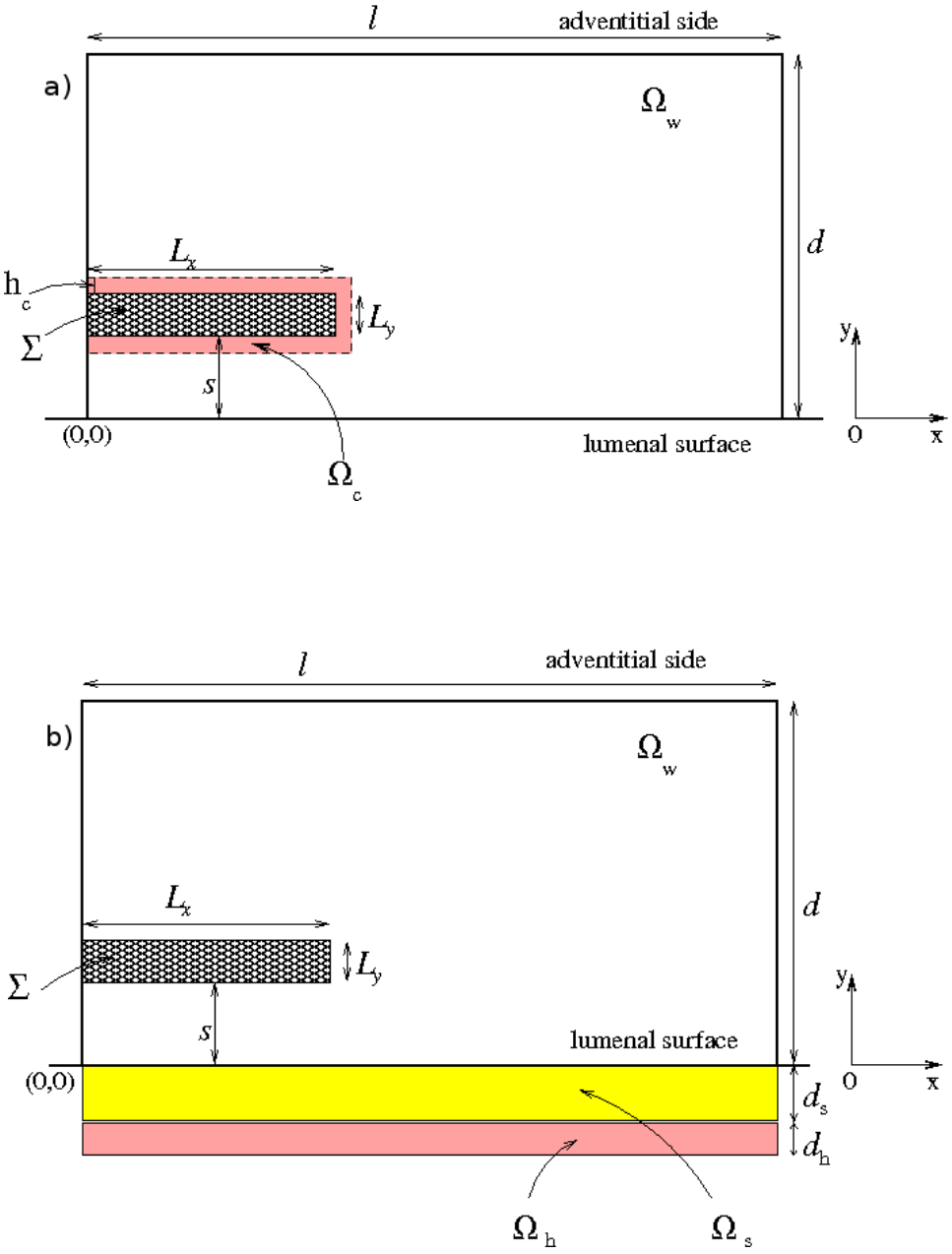

FIGURE 3. Two configurations for drug delivery in DES: a) traditional (top) and b) bi-layer endoluminal gel paving stenting (bottom). The pattern refers to a single embedded half-strut and repeats symmetrically on the left and on the right sides to complete a circular cross section, cfr. Figure 2 (figure elements are not to scale, but share the same dimensions and parameters).

2.2. **Physics.** At the initial time, the drug is contained only in the coating Ω_c and it is uniformly distributed at a maximum concentration C_c and, subsequently released into the wall.

Thus, the dynamics of the drug in the coating is described by the following 2D diffusion equation:

$$\begin{aligned}
&\frac{\partial c_c}{\partial t} - D_c \nabla^2 c_c = 0 && && \text{in } \Omega_c \\
&\nabla c_c \cdot \boldsymbol{n}_c = 0 && \text{(symmetry)} && \text{on } \partial\Omega_c|_{x=0} \\
&\nabla c_c \cdot \boldsymbol{n}_c = 0 && \text{(impermeability)} && \text{on } \partial\Omega_c \cap \partial\Sigma \\
&c_c = C_c && && \text{at } t = 0.
\end{aligned} \tag{1}$$

In the sequel of this work, D will denote the drug diffusivity and $\boldsymbol{n}$ the normal external to the considered medium.

Let us now consider the drug dynamics in the wall. Here mass transfer is not governed by diffusion only, but convection due to the filtration velocity of the plasma may result equally important and a transport term is added. Furthermore we account for a metabolic process (due to drug binding or chemical reaction) and a linear mass consumption is assumed. At adventitial side ($y \to d$), being $d - s \gg L_y$, the concentration c_w at $y = d$ does not change as the time increases and hence it remains equal to its initial value, namely zero. Similarly, $c_w = 0$ at $y = 0$ because of the wash out of the blood stream. Therefore, a fraction of drug is lost in the tissues adjacent to the adventitia and a fraction dispersed in the lumen. Thus, we have the following convection-diffusion-reaction problem:

$$\begin{aligned}
&\frac{\partial c_w}{\partial t} + \nabla \cdot \left(\frac{\alpha_w}{\epsilon_w} \boldsymbol{U}_w \cdot c_w - D_w \nabla c_w \right) + \beta c_w = 0 && && \text{in } \Omega_w \\
&c_w = 0 && \text{(washout or large distance)} && \text{on } \partial\Omega_w\big|_{y=0} \cup \partial\Omega_w\big|_{y=d} \\
&\nabla c_w \cdot \boldsymbol{n}_w = 0 && \text{(symmetry)} && \text{on } \partial\Omega_w\big|_{x=0} \cup \partial\Omega_w\big|_{x=l} \\
&c_w = 0 && && \text{at } t = 0.
\end{aligned} \tag{2}$$

where $\boldsymbol{U}_w$ is a wall volume-averaged plasma filtration velocity, assumed assigned and constant, ϵ_w the wall porosity, $\beta > 0$ a consumption rate coefficient. The coefficient α_w is the so-called tortuosity in the y direction (i.e., the hindrance to drug diffusion imposed by local boundaries).

To close the previous system of equations (1)-(2), the conditions at the coating-wall interface have to be assigned. One of them is obtained by imposing continuity of the mass flux:

$$D_c \nabla c_c \cdot \boldsymbol{n}_c = D_w \nabla c_w \cdot \boldsymbol{n}_w \qquad \text{on } \partial\Omega_c \cap \partial\Omega_w \tag{3}$$

Also, to slow down the drug release rate, a thin film (called *topcoat*) of permeability Π (cm/s) is located at the interface. A continuous mass flux passes through it orthogonally to the coating film with a possible concentration jump. In the present case, the mass transfer through the topcoat can be described using the second Kedem-Katchalsky equation [20, 13]. Thus, the continuous flux of mass passing across the membrane orthogonally to the coating is expressed by:

$$-D_c \nabla c_c \cdot \boldsymbol{n}_c = \Pi(c_c' - c_w') \qquad \text{on } \partial\Omega_c \cap \partial\Omega_w \tag{4}$$

or, alternatively,

$$-D_w \nabla c_w \cdot \boldsymbol{n}_w = \Pi(c_c' - c_w') \qquad \text{on } \partial\Omega_c \cap \partial\Omega_w \tag{5}$$

In equations (4)-(5) the fluid-phase concentration c' is used. This is related to the volume-averaged concentration c through the formula $c' = \dfrac{c}{k\epsilon}$, where ϵ is the porosity and k is the partition coefficient [4]. As one of the last three equations is redundant, we can choose any two of them, for example equations (4) and (5). They apply to all the 3 sides of the coating-wall interface (dashed lines in Fig. 3a).

3. **The bi-layer endoluminal gel paved stenting.** Gel paving is a process in which a biocompatible polymeric solution is applied via catheter to the endoluminal surface of an artery [6, 23]. Accordingly, this procedure implies a narrowing of vessel lumen, and gel thickness should not exceed a given bound in order to prevent unfavorable pressure drop across the paved zone. Moreover the vessel constriction induces a high wall shear stress that could determine premature gel layer erosion with consequent systemic drug release. In order to meet a good erosion resistance on the lumenal side and a proper diffusion inside the artery wall, a double gel layer system is proposed: the inner part (i.e., that faced with artery wall - adventitial side) consists of a soft gel, the outer part (i.e., that in contact with blood stream) exhibits hard gel properties. This set up can be realized, for example, by considering an aqueous polymeric blend solution constituted by a polymer yielding to a soft gel due to temperature increase and an additional polymer yielding to a hard gel due to the addition of a proper crosslinker (i.e., salts) [9]. In other words, body temperature ensures soft gel formation, while the exposition of the outer gel to the crosslinker gives rise to the formation of the thin hard gel layer. It is also assumed that the bi-layer gel does not undergo significant bio-degradation/bio-absorption over the entire drug release period. EGP is realized in conjunction with the insertion of an uncoated stent, which restore the correct blood flow in the stenosed vessel. Stent strut is considered here as a mechanical barrier to the drug released by the gel.

The novel configuration (EGPS) is schematized as in Figure 3b, where subscript s (resp. h) refers to soft gel with domain Ω_s and thickness d_s (resp. hard gel with domain Ω_h and thickness d_h). Differently than in the case of traditional stent, the bi-gel layer prevents convection across the arterial wall, and the governing equation (2.1) now simplifies as:

$$\frac{\partial c_w}{\partial t} - D_w \nabla^2 c_w + \beta c_w = 0 \qquad \text{in } \Omega_w. \tag{6}$$

Due to the absence of metabolic activity in both the soft and hard gel layers, the transport equation pertaining to these domains reduces to the simple diffusion equation:

$$\frac{\partial c_i}{\partial t} - D_i \nabla^2 c_i = 0 \qquad \text{in } \Omega_i \qquad i = h, s. \tag{7}$$

Equations (6) and (7) meet the following requirements:

Boundary conditions along y (across the layers):

$$c_h = 0 \qquad \text{on } \partial\Omega_h\big|_{y=-d_h-d_s} \tag{8}$$

$$D_h \nabla c_h \cdot \boldsymbol{n}_h = D_s \nabla c_s \cdot \boldsymbol{n}_s \qquad \frac{c_h}{c_s} = k_{sh} \qquad \text{on } \partial\Omega_h \cap \partial\Omega_s \tag{9}$$

$$D_s \nabla c_s \cdot \boldsymbol{n}_s = D_w \nabla c_w \cdot \boldsymbol{n}_w \qquad \frac{c_s}{c_w} = k_{sw} \qquad \text{on } \partial\Omega_s \cap \partial\Omega_w \tag{10}$$

$$\nabla c_w \cdot \boldsymbol{n}_w = 0 \quad \text{(impermeability)} \qquad \text{on } \partial\Omega_w \cap \partial\Sigma \tag{11}$$

$$c_w = 0 \quad \text{(large distance)} \qquad \text{on } \partial\Omega_w\big|_{y=d} \tag{12}$$

Boundary conditions along x:

$$\nabla c_i \cdot \boldsymbol{n}_i = 0 \quad \text{(symmetry)} \qquad \text{on } \partial\Omega_i\big|_{x=0} \cup \partial\Omega_i\big|_{x=l} \qquad i = h, s, w. \tag{13}$$

Initial conditions:

$$c_w = 0 \qquad c_s = C_s \qquad c_h = C_h \qquad \text{at } t = 0. \tag{14}$$

where k_{sh} and k_{sw} are, respectively, the hard/soft gel and the soft gel/artery wall partition coefficients.

3.1. **Gel layer thickness estimate.** A fundamental parameter for a correct modelling of diffusive process in EGPS approach is the thickness of the gel layer paving the wall. Indeed, if thick gels are desirable as they can guarantee higher doses and prolonged release (drug dose per unit length is proportional to gel thickness), they can cause an unacceptable pressure drop across the stented zone. In order to estimate the relevant variables, a preliminary fluid dynamical study of the flow over the gel paved portion has been carried out. This analysis allows also the determination of wall shear stress τ, a relevant indicator for the formulation of a suitable erosion resistant gel layer. We consider a portion of coronary artery having a rigid wall (that is a reasonable assumption for a stented coronary) and internal radius R. Let us assume the blood as a viscous fluid with rheological properties governed by a simple power-law viscosity [15]:

$$\eta(\dot{\gamma}) = K\,\dot{\gamma}^{n-1} \tag{15}$$

where K is a model parameter, n the power index, and $\dot{\gamma}$ the shear rate:

$$\dot{\gamma} = \left(\frac{1}{2} tr(\boldsymbol{A}_1^2)\right)^{\frac{1}{2}} \qquad \boldsymbol{A}_1 = \nabla \boldsymbol{v} + (\nabla \boldsymbol{v})^T$$

with $\boldsymbol{v}$ the fluid velocity. In the case of steady and laminar flow, denoting by ρ and P the fluid density and the pressure, the mass and momentum conservation laws are:

$$\begin{aligned} &\nabla \cdot \boldsymbol{v} = 0 \\ &\rho\,(\boldsymbol{v} \cdot \nabla \boldsymbol{v}) = \nabla \cdot \boldsymbol{T} - \nabla P \end{aligned} \tag{16}$$

The equations (16) are solved in the present configuration in a tube of length L, letting as inlet condition a velocity profile obtained by integration of equations (16) in the case of a unstented artery:

$$v(y) = \left(\frac{\Delta P}{2KL}\right)^{\frac{1}{n}} \frac{n}{n+1} R_A^{\frac{n+1}{n}} \left[1 - \left(\frac{y+R}{R_A}\right)^{\frac{n+1}{n}}\right] \qquad -R \le y \le -d_h - d_s. \tag{17}$$

with $R_A = R - d_s - d_h$. The shear stress τ acting on the hard gel can be derived as a component of the stress tensor defined by:

$$\boldsymbol{T} = \eta\,(\dot{\gamma})\,\boldsymbol{A}_1. \tag{18}$$

The analysis of the numerical solution of equations (15)-(16)-(18) allows to correlate gel layer thickness and pressure drop per unit length ($\Delta P/L$). To prevent the onset of a turbulent regime, we found that an acceptable pressure drop per unit length across the stented zone should not exceed 3.5 times that relative to an unstented coronary (see Table 1).

TABLE 1. Dependence of wall shear stress τ and pressure drop/length ($\Delta P/L$) across the gel paved region on total layer thickness.

$d_s + d_h\,(\mu m)$	$\tau(Pa)$	$\Delta P/L(Pa/m)$
0	3.3	4780
220	7.6	16428
250	7.8	19643
275	7.9	23214
300	8.3	28214

4. **Numerical simulations and results.** We are interested in studying the variation of the concentration field in the wall with the geometrical parameters such as the penetration depth s that measures the stent embedding degree, or the mesh length L_x directly related to the void fraction. Our aim is to compare the mass release in the two different configurations of conventional DES (case i) and EGPS (case ii). Comparison is difficult because much of the parameters and the materials are intrinsically related to the specific methodology. However, the following physical values are fixed for computational experiments in both configurations (Fig. 3):

$$d = 0.08cm \qquad l = 0.4cm \qquad L_y = 0.005cm \qquad D_w = 7{\cdot}10^{-8} cm^2/s. \tag{19}$$

The drug mass loaded initially in the coating (case i) and in the gel layers (case ii) (*dose*) is assumed to be equal. All concentrations (considered as averaged mass per area) are nondimensionalized with respect to their initial values ($c \to \dfrac{c}{C_c}$ in the case (i) and $c \to \dfrac{c}{C_h}$ $(C_s = C_h)$ in case (ii)) .

For the conventional stent, the following constants are considered:

$$h_c = 5\mu m \qquad \Pi = 10^{-6} cm/s \qquad D_c = 10^{-10} cm^2/s$$
$$k_c = 1 \qquad k_w = 1 \qquad \epsilon_c = 0.1 \qquad \epsilon_w = 0.61.$$

They have been chosen according to a physical basis and in agreement with the typical scales in DES and data in literature for the coronary arterial wall and heparin drug in the coating layer [4, 11].

In case (ii), preliminary fluid dynamics numerical simulations were independently carried out [5], based on the following set of parameters:

$$n = 0.6, \qquad K = 0.02423\,Pa\,s^{0.6}, \qquad \rho = 1.064\,g/cm^3,$$
$$R = 0.15cm, \qquad L = 1.4cm, \qquad Q = 5.21\,cm^3/s.$$

These values imply a pressure gradient $\Delta P/L = 3296Pa/m$ in equation (17) and a blood pressure P_b upstream the stented region equal to $21331.2Pa\,(160mmHg)$ (such flow rate and pressure values correspond to stressed physiological conditions [10]). The fluid dynamical problem was solved in the steady case with a 2D volume element method (Ansys CFX 10) using a hybrid unstructured mesh and an implicit second order Euler scheme as time integrator. The spatial mesh has been adaptively refined near high gradient region using a number of elements up to 10^6.

Results reveal that a thickening of the total gel layer reflects in an increase of both pressure drop/length ($\Delta P/L$) across the constriction and wall shear stress (τ) as reported in Table 1. The thickness of gel layer has been chosen as $220\mu m$ to guarantee reasonable values for pressure drop and wall shear stress. Interestingly, assuming less exasperated flow conditions ($Q = 1.04cm^3/s$ (this implies $\Delta P/L = 1260Pa/m$ in eq. (3.12)) and blood pressure P_b upstream the constriction equal to $10666Pa(80mmHg)$), we obtained a shear stress $\tau = 2.9Pa$ with $d_s + d_h = 250\mu m$.

The optimal partition between d_s and d_h is related to both drug delivery and mechanical properties. As a matter of fact, while a thinner d_h would reflect in a too weak protection against blood erosive action, a thicker d_h would considerably limit drug diffusion towards arterial wall as drug mobility in the hard gel is very low, if not impossible.

Off-line flow simulations [5] suggest an optimal ratio $d_h/d_s \approx 0.1$, and EGPS system simulations are carried out with the following gel layer thicknesses:

$$d_s = 200\mu m \qquad d_h = 20\mu m$$

and with physical parameters:

$$D_s = 10^{-9}cm^2/s \qquad D_h = 10^{-12}cm^2/s \qquad k_{sh} = 1 \qquad k_{sw} = 1$$

The problem of mass release apparently depends on a large number of parameters, each of them run in a finite range, and there is a variety of different limiting cases. As a matter of fact, they cannot be chosen independently from each other, but they are related by some compatibility condition to give rise a realistic output. A sensitivity analysis is carried out at varying void fraction $l - L_x$ ($L_x = 0.05 \div 0.2cm$) and penetration depth ($s = d/10 \div 9d/10$). The small filtration velocity ($U_w \approx 10^{-6}cm/s$) is inhibited by the hard gel barrier in case (ii) and acts as an unfavorable factor in case (i): therefore it is not considered in this preliminary analysis. Similarly $\beta = 0$, since the metabolic process does not influence the comparison between the two cases.

The numerical problem has been solved by finite element method using COMSOL multiphysics package [3]. The spatial domain has been discretized by a unstructured triangular mesh (having ≈ 1000 elements in Ω_c and ≈ 2200 elements in Ω_w in case (i) and ≈ 1300 elements in Ω_s, ≈ 600 elements in Ω_h and ≈ 600 elements in Ω_w, in case (ii)): the mesh is automatically computed and adaptively adjusted according to the size of each domain. The method uses second order Lagrangian polynomial as shape functions, and a Runge-Kutta integration scheme in time, with an adaptive time step.

Simulations of drug release are carried out for a period of time up to 5 days (120 hours): in Figs. 4 and 5, the concentration levels at three instants are reported. Results indicate that concentration levels in the wall increase up to a maximum level and then decrease exponentially to zero. In EGPS case the drug release is more uniform and significantly slowered; a remarkable amount of drug is retained

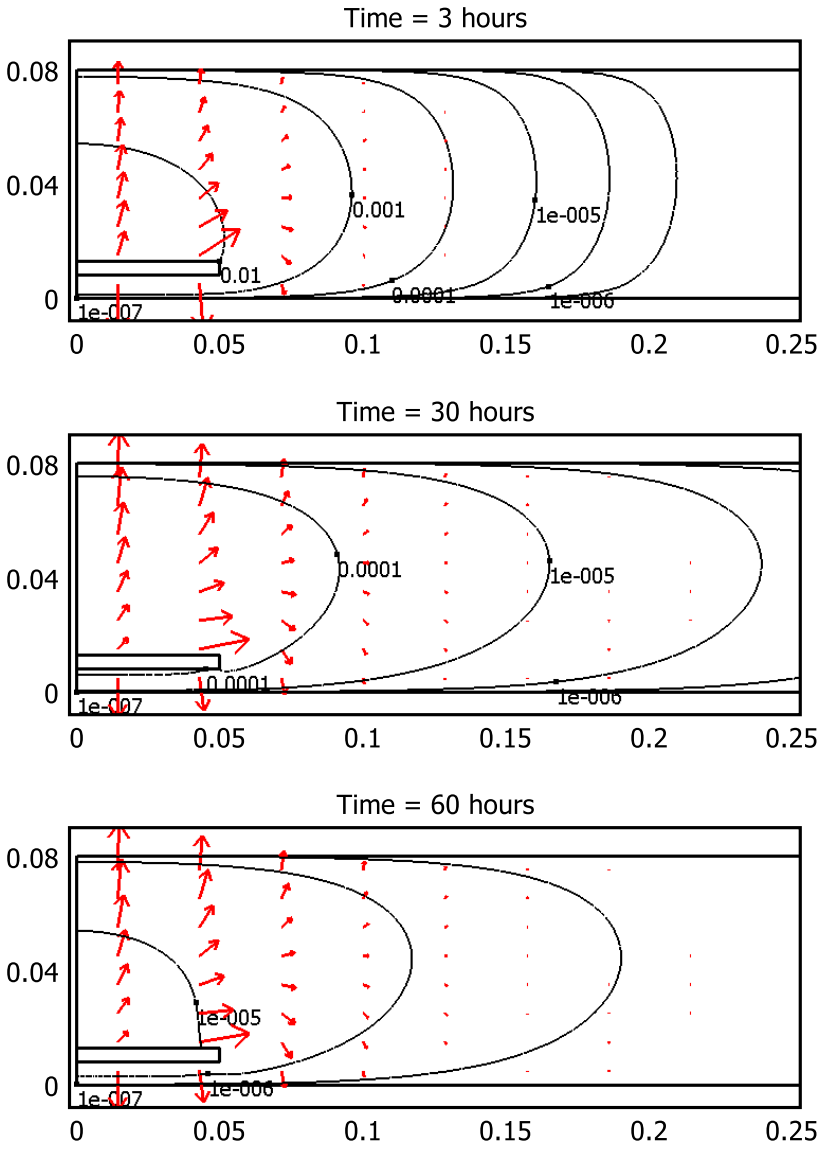

FIGURE 4. Contour lines for concentration in DES case at three instants ($s = d/10$ and $L_x = 0.05\,cm$). In each plot, arrows indicate the magnitude and direction of concentration flux.

in the wall for a considerable time (cfr. contour labels at similar times in Figs. 4 and 5).

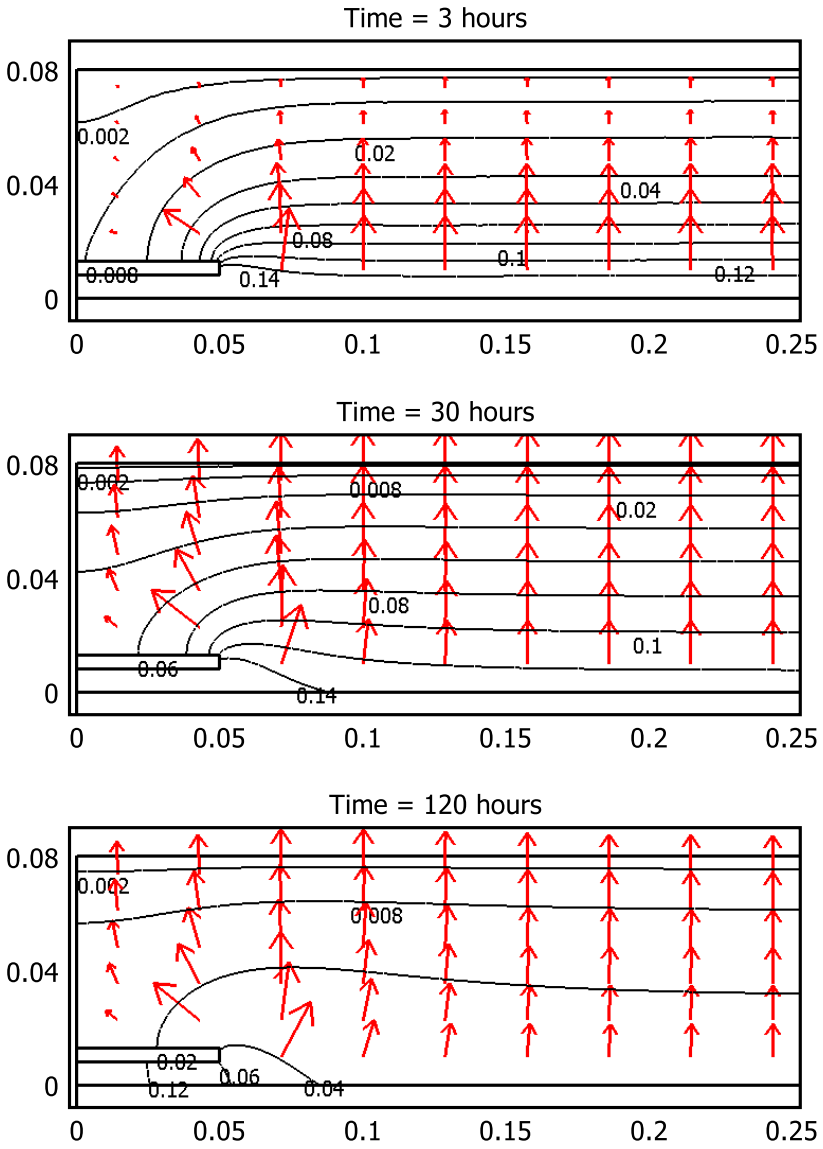

FIGURE 5. Contour lines for concentration in EGPS case at three instants ($s = d/10$ and $L_x = 0.05cm$). In each plot, arrows indicate the magnitude and direction of concentration flux. A more uniform and higher concentration is present in the wall for an extended period of time (cfr. Fig. 4).

The drug mass in the wall is computed as: $M(t) = \int_{\Omega_w} c_w(x, y, t)\, dxdy$ and is referred to the total initial mass: $M(0) = \int_{\Omega_c} c_{tot}(x, y, 0) dxdy = |\Omega_c|$ (case i) and $M(0) = \int_{\Omega_s \cup \Omega_h} c_{tot}(x, y, 0) dxdy = |\Omega_s| + |\Omega_h|$ (case ii).

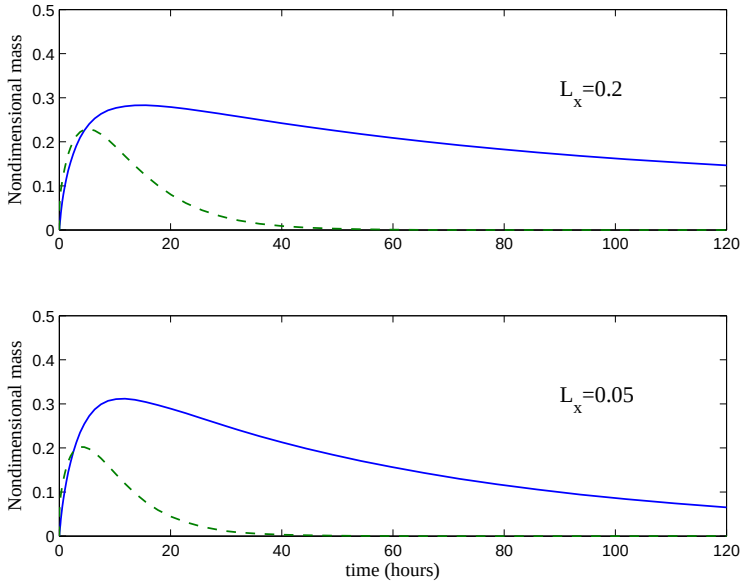

FIGURE 6. Nondimensional mass in the wall as function of time in case of DES (dashed line) and of EGPS (continuous line), for a penetration depth of $s = d/10$. Plots above (a) and below (b) refer to different strut mesh size L_x.

Several test cases are carried out by varying the penetration depth (s) and mesh length (L_x). In Figures 6 and 7 the ratios $\dfrac{M(t)}{M(0)}$ are reported for (i) and (ii) in the limiting cases. Results show that mass in the wall first increase up to a maximum value and then, owing to the absorption at $y = 0$ and at $y = d$, decay exponentially in a finite time.

In the pharmacokinetic characterization of drugs, it is of interest to evaluate to what extent the drugs is distributed and retained in a tissue. This parameter is generally known as *mean residence time* (MRT) and provides a useful insight into the kinetics of a substance released in a porous medium [1]. Roughly speaking, the mean residence time measures the capability of a drug to reside in a tissue, and, for the present application, can be defined as the time that mass in the wall reaches a given percentage of its maximum initial value, say:

$$\mathrm{MRT}_n = \max\left\{M(t) \geq \frac{n}{100} M(0)\right\}$$

or, in other words: $\dfrac{M(\mathrm{MRT}_n)}{M(0)} \simeq \dfrac{n}{100}$. For example, MRT_{10} indicates the time elapsed until the mass in the wall stays above 10% of the maximum initially loaded value. MRT constitutes a quantitative indicator of drug elution used for comparative purposes and for designing novel coating/paving technologies. Actually, for a prolonged therapeutic efficacy, it is important to maximize MRT as a function of some model parameter. For example, from Fig. 6b, it turns out that $\mathrm{MRT}_{10} \simeq 13h$

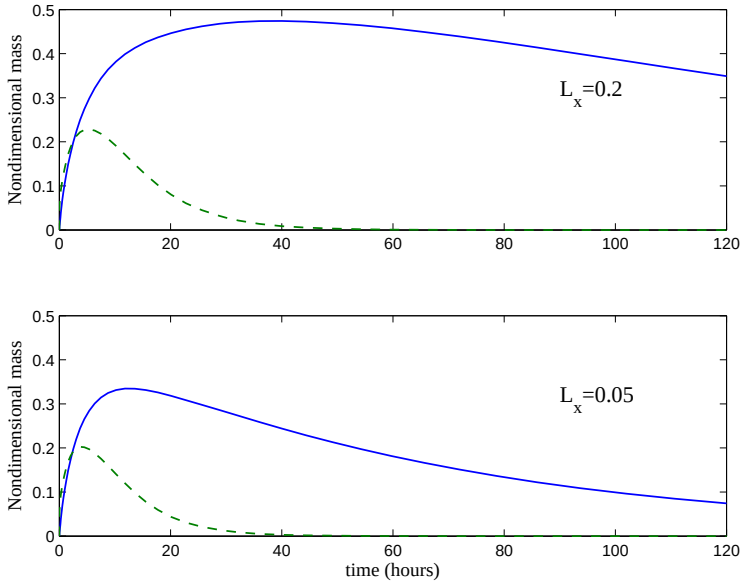

FIGURE 7. Nondimensional mass in the wall as function of time in case of DES (dashed line) and of EGPS (continuous line), for a penetration depth of $s = 9d/10$. Plots above (a) and below (b) refer to different strut mesh size L_x. Differently than traditional DES, the EGP methodology turns out to be more sensitive to geometrical parameters.

in a traditional stent, while $\mathrm{MRT}_{10} \simeq 101h$ in case of EGPS, resulting an increment of nearly 7.5 times.

In the traditional DES (Figs. 6-7, dashed line), a negligible difference is found at varying s and L_x either in MRT and in the peak value, while a tremendous increase of mass is found in EGPS methodology and mass raises considerably with the mesh size L_x and is correlated with the degree of embedding s: a larger strut surface acts as a barrier preventing elution in the tissue and keeping a higher concentration (Figs. 6-7, continuous line). In the comparison of the two drug delivery systems, the peak for M is much higher and occurs at a later instant in EGPS. By examining the EGPS mass release, no appreciable difference is observed with L_x at a lower penetration depth (Fig. 6), whereas a larger value of the peak and a slower drug elution is obtained with a larger mesh size and a deeper insertion (Fig. 7).

Results of drug release in DES are compared with those obtained in an even simpler 1D model [19]. The discrepancy of both concentration field and the mass along a transverse direction is less of 10%. On the other hand, results from this preliminary study indicate that EGPS guarantees a more localized drug elution and reduce systemic losses. In other words, it seems to enable a more *controlled* and *effective* drug release than the traditional coated stents for the treatment of atherosclerosis and restenosis.

5. **Conclusions.** The release of a substance in a living tissue for therapeutic purposes is a common practise in medicine nowadays, through drug delivery devices. In general, the mechanism of release is quite complex and depends on many concurrent biochemical, physical and individual factors. In recent years, new alternative strategies for drug delivery, such as EGPS, are being developed and much effort in modelling is currently addressed to a deeper understanding of the complex drug elution mechanism. This study presents a 2-dimensional approximation model which, as an idealized case, provides a useful tool to predict the fundamental physics of mass transfer and to assess the relative efficacy of the DES and EGPS technology.

Although based on some simplifying assumptions, such as the lowered geometrical dimension, the absence of curvature and the homogeneity of the wall, the model has proved to catch the basic aspects of the release process and is used here for comparative purposes.

More sensitive to the geometrical factors, and tuned in an optimal way, EGPS has been shown to have better capabilities and can be used to design novel efficient drug delivery systems and to improve therapeutic protocols. In addition, the possibility of modulating release rate acting on gel properties regardless of stent characteristics, makes it very versatile and suitable for future improvements related to the discovery of new gels formulation. Finally, should the gel be paved after stent implantation, it is not subject to the considerable stretching present in the polymeric coating of standard DES. These considerations open new perspectives and encourage further investigations of unconventional approaches of drug delivery such as those based on the EGPS technology.

Acknowledgments. This work has been partly supported by the "Fondazione Cassa di Risparmio of Trieste", by the "Fondazione Benefica Kathleen Foreman Casali of Trieste" and by "Fondo Trieste 2006".
The *CNR-Bioinformatics* project is also greatly acknowledged.

REFERENCES

[1] G. Acharya and K. Park, *Mechanisms of controlled drug release from drug-eluting stents*, Advanced Drug Delivery Reviews, **58** (2006), 387–401.
[2] R. M. Califf, *Restenosis: The cost to society*, Am. Heart. J., **130** (1995), 680–684.
[3] COMSOL: http://www.comsol.com
[4] C. Creel, M. Lovich and E. Edelman, *Arterial paclitaxel distribution and deposition*, Circ. Res., **86** (2000), 879–884.
[5] L. Davia, "Simulazione del Processo di Rilascio da uno Stent Medicato," Graduate thesis, Dept. Chemical Eng., Univ. of Trieste, Italy, 2006.
[6] D. S. Eccleston and A. M. Lincoff, *Catheter-based delivery for restenosis*, Advanced Drug Delivery Reviews, **24** (1997), 31–43.
[7] D. L. Fischman, M. B. Leon, D. S. Baim, R. A. Schatz, M. P. Savage, I. Penn, K. Detre, L. Veltri, D. Ricci and M. Nobuyoshi, *A randomized comparison of coronary-stent placement and balloon angioplasty in the treatment of coronary artery disease*, Stent Restenosis Study Investigators, N. Engl. J. Med., **331** (1994), 496–501.
[8] G. Grassi, A. Schneider, S. Engel, G. Racchi, R. Kandolf and A. Kuhn, *Hammerhead ribozymes targeted against cyclin E and E2F1 co-operate to down regulate coronary smooth muscle cells proliferation*, The Journal of Gene Medicine, **7** (2005), 1223–1234.
[9] G. Grassi, A. Crevatin, R. Farra, G. Guarnieri, A. Pascotto, B. Rehimers, R. Lapasin and M. Grassi, *Rheological properties of aqueous pluronic-alginate systems containing liposomes*, Journal of Colloids and Interface Science, **301** (2006), 282–290.
[10] A. C. Guyton and J. E. Hall, "Textbook of Medical Physiology," 11th edition, Elsevier, 2005.
[11] C. Hwang, D. Wu and E. R. Edelman, *Physiological transport forces govern drug distribution for stent-based delivery*, Circulation, **104** (2001), 600–605.

[12] T. C. Jarvis, L. J. Alby, A. A. Beaudry , F. E. Wincott, L. Beigelman, J. A. McSwiggen, N. Usman and D. T. Stinchcomb, *Inhibition of vascular smooth muscle cell proliferation by ribozymes that cleave c-myb mRNA*, RNA, **2** (1996), 419–428.

[13] A. Kargol, M. Kargol and S. Przestalski, *The Kedem-Katchalsky equations as applied for describing substance transport across biological membranes*, Cell. & Molec. Biol. Letters, **2** (1996), 117–124.

[14] L. M. Khachigian, R. G. Fahmy, G. Zhang, Y. V. Bobryshev and A. Kaniaros, *c-Jun regulates vascular smooth muscle cell growth and neointima formation after arterial injury. Inhibition by a novel DNA enzyme targeting c-Jun.*, J Biol. Chem., **277** (2002), 22985–22991.

[15] R. Lapasin and S. Pricl, "Rheology of Industrial Polysaccharides: Theory and Applications," Blackie Academic & Professional, London, 1995.

[16] H. C. Lowe, R. G. Fahmy, M. M. Kavurma, A. Baker, C. N. Chesterman and L. M. Khachigian, *Catalytic oligodeoxynucleotides define a key regulatory role for early growth response factor-1 in the porcine model of coronary in-stent restenosis*, Circ Res., **89** (2001), 670–677.

[17] W. H. Maisel, *Unaswered questions: Drug-eluting stents and the risk of late thrombosis*, New England Journal of Medicine, **356** (2007), 981–984.

[18] F. Migliavacca, F. Gervaso, M. Prosi, P. Zunino, S. Minisini, L. Formaggia and G. Dubini, *Expansion and drug elution model of a coronary stent*, Comp. Meth. Biomech. Biom. Eng., **10** (2007), 63–73.

[19] G. Pontrelli and F. de Monte, *Mass diffusion through two-layer porous media: An application to the drug-eluting stent*, Int. J. of Heat Mass Transf., **50** (2007), 3658–3669.

[20] M. Prosi, P. Zunino, K. Perktold and A. Quarteroni, *Mathematical and numerical models for transfer of low-density lipoproteins through the arterial walls: A new methodology for the model set up with applications o the study of disturbed lumenal flow*, J. Biomech., **38** (2005), 903–917.

[21] F. S. Santiago, H. C. Lowe, M. M. Kavurma, C. N. Chesterman, A. Baker, D. G. Atkins and L. M. Khachigian, *New DNA enzyme targeting Egr-1 mRNA inhibits vascular smooth muscle proliferation and regrowth after injury*, Nat. Med, **5** (1999), 1264–1269.

[22] P. W. Serruys, P. de Jaegere, F. Kiemeneij, C. Macaya, W. Rutsch, G. Heyndrickx, H. Emanuelsson, J. Marco, V. Legrand and P. Materne, *A comparison of balloon-expandable-stent implantation with balloon angioplasty in patients with coronary artery disease*. Benestent Study Group, N. Engl. J. Med., **331** (1994), 489–495.

[23] M. J. Slepian and J. A. Hubbell, *Polymeric endoluminal gel paving: Hydrogel sytems for local barrier creation and site-specific drug delivery*, Advanced Drug Delivery Reviews, **24** (1997), 11–30.

[24] R. Tung, S. Kaul, G. A. Diamond and P. K. Shah, *Narrative review: Drug-eluting stents for the management of restenosis: a critical appraisal of the evidence*, Ann. Intern. Med., **144** (2006), 913–919.

[25] P. Wenaweser, K. Tsuchida, S. Vaina, L. Abrecht, J. Daemen, C. Morger, S. Windecker and P. Serruys, *Late stent thrombosis following drug-eluting stent implantation: Data from a large, two-institutional cohort study*, World Congress on Cardiology, Barcelona, Spain, 2-6 September 2006.

[26] J. L. West and J. A. Hubbell, *Separation of the arterial wall from blood contact using hydrogel barriers reduces intimal thickening after balloon injury in the rat: The roles of medial and luminal factors in arterial healing*, Proc. Natl. Acad. Sci. USA, **93** (1996), 13188–13193.

[27] W. C. Wijns and M. W. Krucoff, *Increased mortality after implantation of first generation drug-eluting stents: Seeing the smoke, where is the fire?*, European Heart Journal, **27** (2006), 2737–2739.

Received February 7, 2008; Accepted February 27, 2009.

E-mail address: mario.grassi@dicamp.units.it;g.pontrelli@iac.cnr.it
E-mail address: teresi@uniroma3.it;ggrassi@units.it;lorycml@libero.it
E-mail address: ferlu1982@libero.it;gigigalax@libero.it